Motion Compensated Coronary MRA using Focused Navigation (fNAV)

Christopher W. Roy[1], John Heerfordt[1,2], Davide Piccini[1,2], Juerg Schwitter[3], and Matthias Stuber[1,4]
[1]*Radiology, Lausanne University Hospital (CHUV) and University of Lausanne (UNIL), Lausanne, Switzerland,* [2]*Advanced Clinical Imaging Technology (ACIT), Siemens Healthcare AG, Lausanne, Switzerland,* [3]*Division of Cardiology and CMR-Center, Lausanne University Hospital (CHUV), Lausanne, Switzerland,* [4]*Center for Biomedical Imaging (CIBM), Lausanne, Switzerland*

Synopsis

Robust visualization of the coronary vessels is challenging due to cardiac and respiratory motion. Several strategies exist that resolve respiratory motion (XD-GRASP) or compensate for it using N-dimensional image-based navigators to correct for N dimensions of motion. We present a novel self-navigation method wherein the minimization of an image metric is used to estimate 3D non-rigid respiratory motion from a 1D navigator signal (focused navigation: fNAV). We validate fNAV for free-breathing cardiac triggered whole-heart CMRA in a realistic numerical phantom, demonstrate its use in cohorts of healthy volunteers and patients, and quantitatively compare fNAV reconstructions to XD-GRASP.

Introduction

Whole-heart Coronary Magnetic Resonance Angiography (CMRA) is typically impeded by cardiac and respiratory motion, requiring ECG gating and respiratory navigation to identify quiescent periods of coronary motion. Unfortunately, physiological variability inherently results in inefficient and unpredictable scan times with a complex setup. Free-breathing CMRA methods without the need for diaphragmatic navigators have been proposed that resolve respiratory motion by binning the data according to an external device or self-navigation signal, and reconstructing with XD-GRASP [1], [2]. Alternatively, respiratory motion can be corrected using either one [3]–[5], two [6], or three-dimensional [7] image navigators to estimate displacement. In general, N dimensional navigators are needed to estimate N dimensions of motion, adding complexity to the MRI acquisition. In this work, we develop a method for estimating 3D respiratory motion from 1D self-navigation signals using an auto-focusing approach we call focused navigation (fNAV). fNAV is based on the assumption that established self-navigation [4] signals are proportional to respiratory displacement as a function of time and the physical amplitude of displacement over either a region of interest or voxel-wise can be estimated through the iterative optimization of a metric for image sharpness [8]–[10]. We validate the proposed technique for free-breathing cardiac triggered whole-heart CMRA in a realistic numerical phantom, demonstrate its use in cohorts of healthy volunteers and patients, and test the hypothesis that 3D voxel-wise respiratory motion correction using fNAV improves coronary vessel sharpness relative to 1D and 3D rigid correction, and XD-GRASP.

Methods

Focused Navigation: The proposed method for fNAV is outlined in Fig. 1 but briefly, cardiac triggered free-breathing whole-heart CMRA data are acquired using 3D radial phyllotaxis sampling with a repeated readout for self-navigation [11]. Self-navigation provides a signal that is proportional to bulk respiratory movement and fNAV posits that the physical displacement of the heart as a function of time in three directions can be estimated by multiplying the self-navigation signal by three amplitudes (A_x, A_y, A_z). The amplitudes are iteratively estimated, k-space is corrected, intermediate images are reconstructed, and a metric for image quality (gradient entropy) calculated either over a region of interest containing the heart for rigid correction or voxel-wise for non-rigid correction is used to determine the optimum values [10]. For comparison purposes, four reconstructions are considered in this work: uncorrected (R_0), 1D rigid correction (R_{1D}), 3D rigid correction (R_{3D}), and finally, voxel-wise 3D non-rigid correction (R_{3Dv}).
Numerical Simulation: To validate fNAV, a realistic numerical simulation was created with matching acquisition parameters to those outlined in Fig. 1 and programable 3D respiratory displacement as well as variable cardiac and respiratory intervals [12], [13]. Eight levels of motion were simulated (Fig. 2) and 20 trials were performed per motion level.
Healthy Volunteer and Patient Data: In vivo data were acquired in 20 healthy volunteers and 32 cardiac patients who provided written informed consent on a 1.5T clinical MRI scanner (MAGNETOM Aera, Siemens Healthcare, Erlangen, Germany) with scan parameters listed in Fig. 1. In addition to the four fNAV reconstructions described in Fig. 1, XD-GRASP (R_{XD}) reconstructions [2] were performed for comparison.
Motion Estimation and Image Evaluation: The optimized fNAV amplitudes were quantitatively compared to the ground truth values across all the levels of simulated motion by computing the Pearson correlation coefficient. fNAV images and motion maps from simulated data were assessed by visual inspection. Qualitative comparison of reconstructions of simulated and in vivo data was performed by visual inspection of reformatted images containing the coronary arteries. Percentage vessel sharpness of the left and right coronary arteries in simulations, volunteers, patients and reconstruction methods was quantified using Soap-Bubble [14] and statistically compared using paired t-tests with the Bonferroni correction.

Results

fNAV motion estimations from numerical data (Fig. 2a) showed a high degree of correlation to the ground truth values in all three dimensions (R=0.99). Similarly, iteratively optimized motion maps generated from fNAV reconstructions of numerical phantom data show good visual agreement with ground truth motion fields in all three dimensions (Fig. 2b). Voxel-wise motion correction (R_{3Dv}) provided the visually sharpest reconstructions as demonstrated by reformatted fNAV reconstructions of the left and right coronary arteries across different levels of simulated motion and showed comparable results to the ground truth reference (Fig. 3). The results of the numerical simulation are echoed by the in vivo data sets (Fig. 4) wherein R_{3Dv} provides the most consistent visualization of the full length of the left and right coronary arteries and shows good agreement with R_{XD} reconstructions. Finally, vessel sharpness measurements in numerical phantom, healthy volunteers, and patient data sets show that in general R_{3Dv} provides the statistically sharpest images (Fig. 5).

Discussion and Conclusion

Focused navigation is a promising technique for improving the quality of free-breathing whole-heart CMRA. This novel approach to respiratory self-navigation can derive 3D non-rigid motion estimations from an acquired 1D signal yielding statistically significant improvement in image sharpness relative to rigid 1D and 3D corrections as well as XD-GRASP reconstructions. This approach, which does not require compressed sensing, may facilitate integration in a clinical environment. However, further study of the diagnostic impact of this technique is warranted to evaluate its full clinical utility.

Acknowledgements

No acknowledgement found.

References

[1] L. Feng, L. Axel, H. Chandarana, K. T. Block, D. K. Sodickson, and R. Otazo, "XD-GRASP: Golden-angle radial MRI with reconstruction of extra motion-state dimensions using compressed sensing," Magn. Reson. Med., vol. 75, no. 2, pp. 775–788, Feb. 2016.

[2] D. Piccini et al., "Four-dimensional respiratory motion-resolved whole heart coronary MR angiography," Magn. Reson. Med., vol. 00, 2016.

[3] C. Stehning, P. Börnert, K. Nehrke, H. Eggers, and M. Stuber, "Free-breathing whole-heart coronary MRA with 3D radial SSFP and self-navigated image reconstruction," Magn. Reson. Med., vol. 54, no. 2, pp. 476–480, 2005.

[4] D. Piccini, A. Littmann, S. Nielles-Vallespin, and M. O. Zenge, "Respiratory self-navigation for whole-heart bright-blood coronary MRI: Methods for robust isolation and automatic segmentation of the blood pool," Magn. Reson. Med., vol. 68, no. 2, pp. 571–579, 2012.

[5] G. Ginami, G. Bonanno, J. Schwitter, M. Stuber, and D. Piccini, "An iterative approach to respiratory self-navigated whole-heart coronary MRA significantly improves image quality in a preliminary patient study.," Magn. Reson. Med., vol. 75, no. 4, pp. 1594–604, Apr. 2016. [6] M. Henningsson, P. Koken, C. Stehning, R. Razavi, C. Prieto, and R. M. Botnar, "Whole-coronary MRI angiography with 2D self-navigated image reconstruction.," Magn. Reson. Med., vol. 67, no. 2, pp. 437–45, Feb. 2012.

[7] N. O. Addy et al., "3D image-based navigators for coronary MR angiography.," Magn. Reson. Med., vol. 77, no. 5, pp. 1874–1883, 2017.

[8] D. Atkinson, D. L. G. Hill, P. N. R. Stoyle, P. E. Summers, and S. F. Keevil, "Automatic correction of motion artifacts in magnetic resonance images using an entropy focus criterion," IEEE Trans. Med. Imaging, vol. 16, no. 6, pp. 903–910, 1997.

[9] R. R. Ingle et al., "Nonrigid autofocus motion correction for coronary MR angiography with a 3D cones trajectory.," Magn. Reson. Med., vol. 72, no. 2, pp. 347–61, Aug. 2014.

[10] J. Y. Cheng, M. T. Alley, C. H. Cunningham, S. S. Vasanawala, J. M. Pauly, and M. Lustig, "Nonrigid motion correction in 3D using autofocusing with localized linear translations.," Magn. Reson. Med., vol. 68, no. 6, pp. 1785–97, Dec. 2012.

[11] D. Piccini, A. Littmann, S. Nielles-Vallespin, and M. O. Zenge, "Spiral phyllotaxis: the natural way to construct a 3D radial trajectory in MRI.," Magn. Reson. Med., vol. 66, no. 4, pp. 1049–56, Oct. 2011.

[12] L. Wissmann, C. Santelli, W. P. Segars, and S. Kozerke, "MRXCAT: Realistic numerical phantoms for cardiovascular magnetic resonance," J. Cardiovasc. Magn. Reson., vol. 16, no. 1, p. 63, Dec. 2014.

[13] C. W. Roy, D. Marini, W. P. Segars, M. Seed, and C. K. Macgowan, "Fetal XCMR: a numerical phantom for fetal cardiovascular magnetic resonance imaging.," J. Cardiovasc. Magn. Reson., vol. 21, no. 1, p. 29, May 2019.

[14] A. Etienne, R. M. Botnar, A. M. C. van Muiswinkel, P. Boesiger, W. J. Manning, and M. Stuber, "Soap-Bubble" visualization and quantitative analysis of 3D coronary magnetic resonance angiograms," Magn. Reson. Med., vol. 48, no. 4, pp. 658–666, Oct. 2002.

Figures

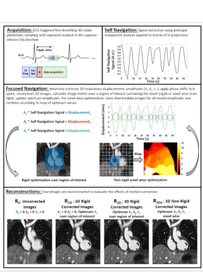

Fig. 1 Schematic diagram of focused navigation framework. A prototype 3D bSSFP sequence with radial phyllotaxis sampling was employed with RF excitation angle: 90° non-selective, TR/TE: 3.14/1.57 ms, spatial resolution: (1.1 mm)3 [4], [11].

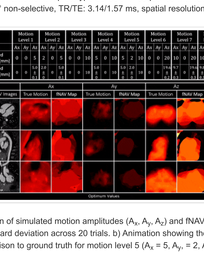

Fig. 2 Numerical phantom results. a) Comparison of simulated motion amplitudes (A_x, A_y, A_z) and fNAV estimates across 8 different motion levels. Each fNAV estimation represents the mean and standard deviation across 20 trials. b) Animation showing the iterative optimization of fNAV motion maps and comparison to ground truth for motion level 5 (A_x = 5, A_y, = 2, A_z = 10).

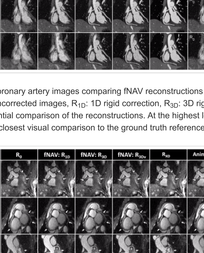

Fig. 3 Animated figure showing reformatted coronary artery images comparing fNAV reconstructions of numerical phantom data to the ground truth reference for increasing levels of motion. R_0: uncorrected images, R_{1D}: 1D rigid correction, R_{3D}: 3D rigid correction, and R_{3Dv}: voxel-wise 3D non-rigid correction. The animated frame provides a sequential comparison of the reconstructions. At the highest level of simulated motion, R_{3Dv} clearly provides the closest visual comparison to the ground truth reference.

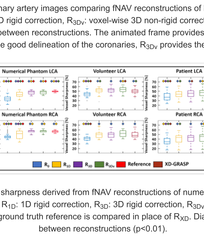

Fig. 4 Animated figure showing reformatted coronary artery images comparing fNAV reconstructions of healthy volunteer and patient data to XD-GRASP. R_0: uncorrected, R_{1D}: 1D rigid correction, R_{3D}: 3D rigid correction, R_{3Dv}: voxel-wise 3D non-rigid correction, and R_{XD}: XD-GRASP reconstruction. Arrows denote regions where coronary visibility varies between reconstructions. The animated frame provides a sequential comparison of the reconstructions. While R_{1D}, R_{3D}, and R_{XD} provide good delineation of the coronaries, R_{3Dv} provides the best overall vessel conspicuity.

Fig. 5 Quantitative evaluation of coronary vessel sharpness derived from fNAV reconstructions of numerical phantom (N=160), healthy volunteer (N=20), and patient data (N=32). R_0: uncorrected images, R_{1D}: 1D rigid correction, R_{3D}: 3D rigid correction, R_{3Dv}: voxel-wise 3D non-rigid correction, and R_{XD}: XD-GRASP reconstruction. For simulated data, the ground truth reference is compared in place of R_{XD}. Diamonds denote statistically significant differences between reconstructions (p<0.01).